Research Square

Preprints are preliminary reports that have not undergone peer review.
They should not be considered conclusive, used to inform clinical practice,
or referenced by the media as validated information.

Proteome Profiling of Intestinal Cultures Treated with Bacteroides fragilis Vesicles Reveals Insights into the Anti-Inflammatory Response

Natalya B. Zakharzhevskaya

natazaha@gmail.com

Lopukhin Federal Research and Clinical Center of Physical-Chemical Medicine of Federal Medical Biological Agency

Olga Yu. Shagaleeva

Lopukhin Federal Research and Clinical Center of Physical-Chemical Medicine of Federal Medical Biological Agency

Olga V. Pobeguts

Lopukhin Federal Research and Clinical Center of Physical-Chemical Medicine of Federal Medical Biological Agency

Daria S. Matyushkina

Scientific Research Institute for Systems Biology and Medicine, Moscow, Russia

Daria A. Kashatnikova

Lopukhin Federal Research and Clinical Center of Physical-Chemical Medicine of Federal Medical Biological Agency

Dmitry A. Kardonsky

Lopukhin Federal Research and Clinical Center of Physical-Chemical Medicine of Federal Medical Biological Agency

Elizaveta A. Vorobeva

Lopukhin Federal Research and Clinical Center of Physical-Chemical Medicine of Federal Medical Biological Agency

Artemiy S. Silantiev

Lopukhin Federal Research and Clinical Center of Physical-Chemical Medicine of Federal Medical Biological Agency

Viktoria D. Kazakova

Lopukhin Federal Research and Clinical Center of Physical-Chemical Medicine of Federal Medical Biological Agency

Irina V. Kolesnikova

Lopukhin Federal Research and Clinical Center of Physical-Chemical Medicine of Federal Medical Biological Agency

Anna A. Vanyushkina
Skolkovo Institute of Science and Technology
Andrei V. Chaplin
Lopukhin Federal Research and Clinical Center of Physical-Chemical Medicine of Federal Medical Biological Agency
Irina V. Podoprigora
Peoples' Friendship University of Russia (RUDN University)
Boris A. Efimov
Lopukhin Federal Research and Clinical Center of Physical-Chemical Medicine of Federal Medical Biological Agency

Research Article

Keywords: Bacteroides, OMVs, HT-29, SW837

Posted Date: July 27th, 2026

DOI: https://doi.org/10.21203/rs.3.rs-10447000/v1

License: This work is licensed under a Creative Commons Attribution 4.0 International License.
Read Full License

Additional Declarations: No competing interests reported.

Abstract

The gut is under complex attack by a large number of biologically active molecules, including bacterial enzymes, metabolites, nucleic acids and immunoactive compounds. Most of these components are present in outer membrane vesicles (OMVs), which are actively produced by all bacterial types. *Bacteroides fragilis*, a member of the gut microbiota, has unique OMV components that are known to have both pathogenic and positive immunomodulatory properties. The OMVs of *Bacteroides fragilis* are well characterized by proteomic and metabolomic methods and therefore represent a suitable comprehensive framework for assessing the overall molecular impact of bacterial OMVs on intestinal cultures. We studied proteomic changes in colon (HT-29) and rectal (SW837) adenocarcinoma cell lines treated with OMVs isolated from the enterotoxigenic *Bacteroides fragilis* BOB25 strain (ETBF) and the nontoxigenic *Bacteroides fragilis* JIM10 strain (NTBF). The cell lines were incubated with ETBF and NTBF OMVs for three and five hours, after which the total proteomes of the cell lines were isolated and annotated via 2D electrophoresis, followed by mass spectrometric identification of proteomic differences. As a result, the SW837 cell line showed a more significant range of proteome differences than the HT-29 cell line, including not only up- and downregulated proteins involved in cytoskeletal reorganization and cell adhesion but also proteins involved in cell proliferation and the proinflammatory response. We found that SW837 cells treated with NTBF OMVs characterized by high amount of IL18, which plays a profound role in the initiation phase of the immune response by recruiting dendritic cells (DCs). The ETBF OMVs demonstrated the simultaneous coexistence of cell proliferation- and apoptosis-promoting factors. We hypothesize that both types of OMVs may contribute to the observed anti-inflammatory effects, as the same proteins were found to be affected in cell lines treated with ETBF and NTBF OMVs. However, the presence of toxins in ETBF OMVs may delay anti-inflammatory activity until the cell has fully repaired the damaged cytoskeleton.

INTRODUCTION

The microbiota is characterized by multiple symbiotic relationships with the host, providing a protective nutritional niche for bacteria, while bacterial metabolites are involved in host metabolism [1]. The investigation of intercellular communication between the most abundant bacterial species and intestinal cells is a priority for a comprehensive assessment of molecular cell effects contributing to health and pathology [2]. *Bacteroides*, which constitute up to 25% of all anaerobic bacteria, are highly functional and promote the degradation of chondroitin sulfates, heparin and glycosphingolipids [3–5]. Mucin hydrolysis contributes to the formation of glycans and sialic acids, which are actively taken up by commensal bacteria as a nutritional component [6]. *Bacteroides fragilis*, a member of the genus *Bacteroides*, is also involved in the biotransformation of bile acids and the proteolytic degradation of proteins [7]. The uniqueness of the *Bacteroides fragilis* species is determined by the possibility of pathogenic and nonpathogenic strains coexisting [8]. A genomic study of toxigenic (BOB25) and nontoxigenic *Bacteroides fragilis* strains (JIM10) revealed minor differences, including the presence of a small pathogenicity island containing the toxin fragilysin in the BOB25 genome [9]. Fragilysin cleaves E-cadherin, the major protein involved in intercellular contacts. E-cadherin degradation contributes to

reversible cell rounding and separation [10, 11]. E-cadherin degradation has been demonstrated in the HT29/C1 cell line treated with fragilysin [8]. In addition, toxin-induced intestinal permeability promotes the release of the proinflammatory cytokines interleukin-8, epithelial neutrophil-activating protein 78 (ENA-78), monocyte chemotactic protein (MCP-1), and growth-associated oncogene α (GRO-α), also called CXCL [12]. Fragilysin-treated cells also secrete the inactive form of transforming growth factor β (TGF-β), which is necessary for mucosal repair [12]. According to the literature, the pathogenic strains of *Bacteroides fragilis* (ETBF) are not only associated with intestinal inflammation but also involved in neoplastic transformation [13].

Nonpathogenic *Bacteroides fragilis* strains (NTBFs) are characterized by polar to ETBF properties [14]. Surface-located polysaccharide A (PSA) has been shown to have immunomodulatory effects [15]. PSA interacts with TLR2 receptors on dendritic cells, promoting IL10 secretion. IL10 modulates the activity of CD4 + FOXP3+ regulatory T cells (Tregs), which suppress inflammation [16]. The secretory potential of *Bacteroides fragilis* can be realized through an extremely small number of mechanisms. To date, 6 types of secretions have been described for bacteria, of which *Bacteroides fragilis* has been confirmed to have only the sixth type of bacterial secretion. However, *Bacteroides*, the most common type of bacteria, can also secrete outer membrane vesicles (OMVs) [9, 17, 18]. The primary involvement of OMVs in the process of external secretion of *Bacteroides* has been confirmed [14]. The enzymatic hydrolase activity of OMVs has also been demonstrated [19]. Further detailed proteomic analysis revealed the presence of five enzyme classes and different structural proteins in *Bacteroides fragilis* OMVs, as well as metabolites that were demonstrated to be involved in biochemical reactions [20]. Fragilysin was also shown to be associated with OMVs, suggesting that vesicles are involved in the secretion and delivery of the toxin to target cells [9].

After a detailed proteome and metabolome annotation of the OMV composition, an analysis of the molecular effects of OMV-treated cultured cells seems to be interesting [21]. It has been shown that PSA is also located on the surface of vesicles, suggesting that OMVs are directly involved in the described immunomodulatory effects [22]. However, a comprehensive assessment of the influence of OMVs on epithelial cultures is scarce in the literature. Considering all previously observed effects of individual components of OMVs, we used two-dimensional electrophoresis followed by mass spectrometric identification of protein differences to provide an overview of the proteomic response of the most commonly used colorectal cancer cell lines of colon (HT-29) and rectal (SW837) adenocarcinoma cell lines, treated with ETBF and NTBF OMVs.

RESULTS

OMV isolation and morphological evaluation of Bacteroides

OMVs were isolated by the standard method using filtration and ultracentrifugation. The prepared samples were analyzed by NTA and TEM. TEM was used to analyze the morphology of the OMVs. This

negative contrast allowed us to identify a significant number of OMVs in the preparations of both strains. According to a number of publications, the size of vesicles can range from 20 to 150 nm for different bacteria relative to their size. The expected size of the *Bacteroides* vesicles was between 20 and 80 nm. By visual assessment of approximately 1000 vesicles in different ETBF and NTBF OMV preparations, the OMV size was determined to range from 20 to 120 nm (Fig. 1a). To clarify the size and concentration of the OMVs, the NTA method was used. The particle concentrations are shown in Fig. 1b. The hydrodynamic size of the ETBF and NTBF vesicles was 117 ± 4 nm for the ETBF OMVs and 96 ± 3 nm for the NTBF OMVs (Fig. 1c).

Western blot analysis of ETBF vesicle enzymatic activity

The isolated OMVs (NTBF and ETBF) were separated by SDS—PAGE to confirm the characteristic spectra of the proteins (Fig. 2a). The degradation of E-cadherin was confirmed by treating the HT-29 cell line with ETBF OMVs containing toxins [12]. The same effect of ETBF OMVs containing toxins on cellular E-cadherin was also observed in SW837 cell culture. The SW837 cell line was treated with ETBF OMVs at a final concentration of 5×10^13 particles/ml for 15 minutes and for two hours. After two hours, E-cadherin was completely degraded in the SW837 cell line treated with ETBF OMVs. No effect on E-cadherin structure was observed in the SW837 culture treated with NTFB OMVs (Fig. 2b).

Proteomic annotation of the cellular effects promoted by ETBF and NTBF OMVs

A viability assay of SW 837 cells treated with OMVs was carried out before proteomic analysis. Data on the viability of HT-29 cells treated with *Bacteroides fragilis* OMVs are available [25]. Despite the effect of the established toxin on the E-cadherin structure, no significant number of dead cells were observed in cell culture after 5 hours of ETBF OMV treatment. We analyzed the viability of SW 837 cells treated with different concentrations of OMVs ranging from 0.05 to 5×1013 particles/ml (Fig. 2c). No dose-dependent effect was observed with increasing OMV concentrations. The maximal tested OMV concentration (5×1013 particles/ml) was chosen for further experiments.

To reveal the molecular effects of bacterial vesicles, we performed proteomic analysis of HT-29 and SW 837 cell lines treated with ETBF and NTBF OMVs using 2D differential electrophoresis followed by identification of proteomic differences via time-of-flight mass spectrometry. The cutoff score for protein identification in the Mascot engine was 44 ($p < 0.05$). A protein was identified as significantly altered if the fold change was greater than 2 (upward and downward). First, the proteomic effects of ETBF and NTBF OMVs on the HT-29 cell line were compared. Despite the expected range of molecular effects, no proteomic differences were detected in the HT-29 cell line treated with ETBF and NTBF OMVs. Proteomic differences obtained by two-dimensional electrophoresis are shown in **Figure S1**. We detected up- and downregulated proteins in the HT-29 cell line treated with ETBF and NTBF OMVs for 5 hours, which could be divided into several groups according to their functional activity. Group A included proteins related to

the cell cytoskeleton, tubulin alpha-1B chain, keratin type II cytoskeletal 8, kallikrein 8, and calpain-8. As shown in **Figure S1**, all the above-mentioned proteins were downregulated in HT-29 cells treated with both ETBF and NTBF OMVs, indicating the involvement of cytoskeletal components in cell-OMV interactions. On the other hand, proteins and chaperones, referred to as group B in **Figure S1**, were upregulated in the HT-29 cell line treated with ETBF and NTBF OMVs. We observed relative stability of the HT-29 cell line after treatment with ETBF and NTBF OMVs. In this regard, the experiment was continued with the SW-837 cell line.

More proteomic changes were found in SW-837 cell lines treated with ETBF and NTBF OMVs. Comparative proteomic analysis of SW837 cell lines treated with NTBF OMVs (Fig. 3) and ETBF OMVs (Fig. 4) for 3 and 5 hours revealed significant proteomic differences between treated and untreated cell lines, which can be divided into several groups according to their functional activity (**Supplementary Table S1-S4**).

Major proteomic differences were observed in SW-837 cells treated with NTBF OMVs for 3 hours for proteins involved in cytoskeleton reorganization and cell proliferation (Fig. 3).

A complete list of the proteins that were dysregulated in the SW 837 cell line after treatment with NTBF OMVs for 3 hours and protein functional annotation is provided in **Supplementary Table S1**. The most important up- and downregulated proteins that were observed in SW-837 cells treated with NTBF OMVs for 3 hours were SNN, SPB5, DTX and ARPC2. All of these proteins are involved in cell proliferation, the activation of fundamental pathways, such as the MAPK and ERK signaling pathways, and the activation of interferon-I-mediated inflammatory pathways.

Proteomic changes in the SW-837 cell line treated with NTBF OMVs for 5 hours continued to increase (Fig. 3). We observed up- and downregulated proteins that are responsible for cell proliferation. Chaperones and proteins involved in carbohydrate metabolism were also upregulated. At the same time, the number of proteins involved in cytoskeleton reorganization decreased. The following proteins were found to be the most important in the SW-837 cell line treated with NTBF OMVs for 5 hours: Nucleophosmin, Serpin B3 and IL18.

Serpin B3 modulates the host immune response against tumor cells. Nucleophosmin is implicated in a number of pathways, including mRNA transport, chromatin remodeling, apoptosis and genome stability. IL18 is a proinflammatory cytokine that is primarily involved in epithelial barrier repair and polarized T-helper 1 (Th1) cell and natural killer (NK) cell immune responses. All of these proteins were upregulated. Additionally, the expression level of cytokine genes encoding IL18, IL10 and a number of other cytokines was determined. Sequence of primers used in real-time PCR are listed in **Supplementary Table S8.** According to the data obtained the expression level of IL8, IL18, IL10 and serpin B3 were differed between ETBF or NTBF OMVs treated and untreated SW-837 cell line (**Figure S2**).

A complete list of the proteins that were dysregulated in the SW 837 cell line treated with NTBF OMVs for 5 hours and protein functional annotations is provided in **Supplementary Table S2**.

Proteomic changes were also observed in SW-837 cell lines treated with ETBF OMVs for 3 hours (**Supplementary Table S3**). Notably, a greater number of proteins were dysregulated in the SW-837 cell line treated with NTBF OMVs than in the SW-837 cell line treated with ETBF OMVs. The most dysregulated proteins were involved in cell cytoskeleton reorganization and cell proliferation (Fig. 4).

However, the cytoskeletal proteins were multidirectional regulated in the cultures treated with both types of OMVs. Among all the cytoskeletal proteins, the downregulated MAPRE1 protein was particularly interesting. According to the literature, its overexpression has been found to induce nuclear accumulation of beta-catenin and activation of the beta-catenin/T-cell factor pathway, leading to the promotion of cell growth. Apparently, downregulated MAPRE1 protein expression in cultures treated with ETBF OMVs had the opposite effect. Proteins that are responsible for cell adhesion and Golgi apparatus function were also dysregulated. Proteins responsible for proteasome degradation were upregulated in the SW-837 cell line treated with ETBF OMVs. A complete list of the proteins that were dysregulated in the SW 837 cell line after treatment with ETBF OMVs for 3 hours and protein functional annotation is provided in **Supplementary Table S3**.

After 5 hours of ETBF OMV treatment, proteomic changes in the SW-837 cell line continued to increase, as did those in the SW-837 cell line treated with NTBF OMVs (Fig. 4). We observed up- and downregulated proteins responsible for cell proliferation, proteasome degradation, carbohydrate and protein metabolism and chaperone activity. The following proteins were found to be the most important for the total cellular response in the SW-837 cell line treated with ETBF OMVs for 5 hours: NPM MAPRE1 and HSPB1. Interestingly, these proteins were upregulated in the SW-837 cell line treated with NTBF OMVs for 3 hours. Both types of OMVs likely promote similar molecular effects in the SW837 cell line. However, in the SW-837 cell line treated with ETBF OMV, these cellular effects may be delayed, possibly due to the presence of the toxin. A complete list of the proteins that were dysregulated in the SW 837 cell line after treatment with ETBF OMVs for 5 hours and protein functional annotation is provided in **Supplementary Table S4**.

Cell Signaling Pathways associated with ETBF and NTBF OMVs

Potential pathways involved in the overall cellular response in SW837 cell lines treated with *Bacteroides fragilis* OMVs were assessed (**Supplementary Table 5–7**). Pathways that were involved in SW837 cell line response to the NTBF OMVs treatment for 3 and 5 hours are represented in Fig. 5 **(a, b)**. Only the cell-extracellular matrix interaction pathway was involved in the SW837 cell line response to the NTBF OMVs treatment with for 3 hours (Fig. 5c). However, more than 30 different interaction pathways, including key pathways such as immune system (HSA-168256), infectious disease (HSA-5663205), and Rap1 signaling (HSA-392517), transcriptional regulation by TP53 (HSA-6791312), vesicle-mediated transport (HSA-5653656), antigen presentation: folding, assembly and peptide loading of class I MHC (HSA-983170) and others (Fig. 5d), were involved in the SW837 cell line treatment by with NTBF OMVs for 5 hours.

Interestingly, the SARS-CoV-1 and SARS-CoV-2 infection pathways were also involved in complex cell response to the NTBF OMVs treatment, possibly due to the same cellular targets for OMVs and viruses.

The total number of pathways that were involved in the cell response to the ETBF OMVs treatment was significantly less than that in the culture treated with NTBF OMVs (Fig. 6a, 6b). More pathways were expected in the cultures treated with ETBF OMVs because of the presence of toxins. However, the only pathway of protein processing in the endoplasmic reticulum (HSA 04141) was observed in the SW837 cell line treated with ETBF OMVs for 3 hours (Fig. 6c). Dysregulated proteins were involved in more than 15 different interaction pathways, including the antigen processing and presentation pathway (HSA04612), apoptosis pathway (HSA-109581), immune pathway (HSA-168256) and innate immune system pathway (HSA-168249), in the cell lines treated with ETBF OMVs for 5 h (Fig. 6d).

The pathways most significantly involved in cell lines response in culture treated with ETBF OMVs were MAPK6/MAPK4 signaling (HSA-5687128) and negative regulation of NOTCH4 signaling (HSA-9604323). Association of these pathways likely occurs in cell lines treated with *Bacteroides fragilis* toxin. Among all pathways observed in cell lines treated with ETBF and NTBF OMVs, common pathways were identified: antigen processing and presentation (hsa04612), infectious disease (HSA-5663205), regulation of mRNA stability by proteins that bind AU-rich elements (HSA-450531), and immune system (HSA-168256) pathways. There is a clear tendency to associate cellular pathways involved in the immune response to OMV attack. Cytoskeleton repair and subsequent involvement of immune response pathways are prioritized in cells treated with toxin-containing OMVs (ETBF OMVs). For example, the FLNA and FBLIM1 proteins, which are involved in the cell-extracellular matrix interaction pathway, were downregulated in the SW837 cell line treated with ETBF OMVs for 5 hours compared with the culture treated with NTBF OMVs.

DISCUSSION

A number of studies have demonstrated the ability of bacterial vesicles to fuse with eukaryotic membranes, facilitating the penetration of OMVs into the cell [26–28]. The overall biological effects observed in OMV-treated cultures may contribute to the discovery of new mechanisms of host-microbiota interactions. However, preliminary proteomic and metabolomic characterization of bacterial vesicles may be useful for detailed functional annotation of molecular cellular effects after treatment with OMVs. A previous study dedicated to proteome and metabolome annotation of *Bacteroides fragilis* OMVs was continued by studying the proteomic effects of OMV-treated cell lines [9].

Initially, the quality and concentration of the isolated vesicles were assessed by using TEM and NTA methods. We confirmed that the morphology and concentration of the isolated OMVs were in complete agreement with both the literature and our previously published data. [21]. As ETBF has previously been shown to secrete a vesicle-associated toxin, SW837 cells were treated with ETBF OMVs [29]. As a result, time-dependent E-cadherin degradation was also confirmed in the SW837 cell line, as previously observed in the HT-29 cell line [25]. Although OMVs containing toxins contributed to E-cadherin

degradation, vesicles had no effect on the morphology or viability of the cells. It is important to note that isolated toxins contribute to reversible cell rounding and separation [10, 11]. Perhaps the destructive effects of the toxin on cellular physiology are compensated by the action of other proteins. Previously, the secretome of HT-29 cells treated with the isolated *Bacteroides fragilis* toxin has been fully described [25]. The number of proteins that were dysregulated in the cell line treated with the toxin was minimal compared to that in the untreated cell line (approximately 20–30 proteins). ETBF OMVs contain more than 300 proteins, including enzymes, and we expected to observe a large number of molecular effects in HT-29 cells treated with ETBF OMVs. However, the same numbers of proteins were found to be up- and downregulated in HT-29 cells treated with ETBF or NTBF OMVs for 5 hours. We found that proteins belonging to the cell cytoskeleton (tubulin alpha-1B chain, keratin type II cytoskeletal 8, kallikrein 8, and calpain-8) were downregulated, but heat shock protein chaperones were upregulated in both HT-29 cell lines treated with ETBF and NTBF OMVs. The identified mitochondrial heat shock protein (60 kDa) is responsible for the folding of new proteins that enter cells and may be involved in the processes of recognition and subsequent proteasomal degradation of newly arrived bacterial proteins [30]. Thus, the major differences were observed only in a group of cytoskeletal proteins. No direct effect of the toxin associated with ETBF OMVs on the proteome of the HT-29 cell line was detected. This result likely indicates that the HT-29 cell line may not be fully accessible for bacterial vesicles due to the presence of a surface mucin layer [31].

The SW-837 cell line was treated with ETBF and NTBF OMVs for 3 and 5 hours. We chose this time period for our experiment because we believe that the interaction time between OMVs and intestinal cells coincides with the time of normal intestinal motility [32]. Therefore, we expected to detect proteomic effects in cell cultures treated with OMVs for 3 hours and to observe the described effects after 5 hours of OMV exposure.

It was possible to identify up- and downregulated proteins, which are characteristic of cellular responses from cell differentiation to cell apoptosis, in SW-837 cells treated with NTBF OMVs for 3 hours. Among the identified proteins were cytoskeletal components and structural proteins of the Golgi apparatus, cell adhesion proteins, proteins responsible for proteasomal degradation and enzymes active in the processes of cell proliferation and transformation. According to the data obtained, cytoskeleton reorganization occurred for the first three hours in cultures treated with ETBF or NTBF OMVs. If some cytoskeletal proteins can be involved in the process of cellular uptake of bacterial vesicles, then other proteins, such as ACTG, could be immediately associated with cell proliferation or apoptosis [33]. Upregulated heat shock proteins are also involved in cytoskeletal reorganization [34]. Despite a number of proteomic changes, only a few groups of proteins were differed in amount in cell lines treated with ETBF and NTBF OMVs for 3 hours. Cell-extracellular matrix interaction (HSA-446353) and protein processing in the endoplasmic reticulum (hsa04141) signaling pathways were involved cell response in cell lines treated with NTBF or ETBF OMVs, respectively. Proteins that were involved in the HSA-446353 pathway are directly involved in the reorganization of the cytoskeleton, probably due to cell and vesicle membrane fusion.

However, it is also interesting to observe up- and downregulated proteins that were different in cultures treated with ETBF or NTBF OMVs for 3 hours and were not associated with signaling pathways. The proteins SNN, SPB5, DTX and ARPC2 were upregulated in the SW837 cell line treated with NTBF OMVs for 3 hours. SERPINB5 is involved in cell matrix organization and the regulation of epithelial cell proliferation and blocks tumor growth, invasion and metastasis [35]. Increased SERPINB5 expression was associated with a worse prognosis in patients with colorectal cancer [36]. The upregulation of SERPINB5, which was found in cultures treated with NTBF OMVs, may indicate the intensification of cell proliferation, which can generally be a positive vital effect for cells. The ARPC2 protein, which forms the basis of the Arp2/3 protein complex, is involved in the process of actin polymerization in cells [37–38]. To date, there is no clear link between this protein and colorectal cancer, but there is evidence that the ARPC2 protein is overexpressed in gastric cancer. The ARPC2 protein is also involved in cell proliferation and invasion [39]. Thus, similar to SERPINB5, the ARPC2 protein may promote cell survival when cells are treated with NTBF OMVs. DTX4 was also upregulated in cell cultures treated with NTBF-OMVs. DTX is a ubiquitin ligase and promotes the degradation of the TBK1 protein, a participant in the interferon-I-mediated inflammatory pathway [40]. The inflammatory process is initiated by innate immune cells via pathways such as the NF-κB-, MAPK- and type I interferon (IFN-I)-mediated inflammatory pathways. Pattern recognition receptors are intracellular NLR receptors, and genetic mutations in the NOD2 gene, for example, are associated with susceptibility to Crohn's disease [41]. NLRs are known to indirectly regulate NF-κB and MAPK pathway activation through the subsequent secretion of cytokines, chemokines and IFN. DTX4 protein, which is overexpressed in cell lines treated with NTBF OMVs, may increase the amount of active ubiquitin-associated degradation of TBK1, leading to decreased activity of the interferon-mediated inflammatory pathway. Interestingly, *Bacteroides fragilis* vesicles reduce the inflammatory response by PSA-mediated immune suppression [42]. It is likely that the overall anti-inflammatory effect of vesicles may involve several molecular mechanisms activated during interactions between OMVs and cells. The observed DTX4 overexpression in cell lines treated with NTBF OMVs could be a result of PSA-mediated immune suppression or a consequence of the influence of unknown bacterial proteins on the target cells. Stannin (SNN), a highly conserved 88 amino acid protein, is associated with cell membranes and is partially localized in the mitochondria. SNN simultaneously regulates components of the MAPK and ERK signaling pathways, which are important for cell proliferation [43]. SNN was upregulated in cell lines treated with NTBF OMVs. STRAP also activates the MAPK/ERK signaling pathway and reduces the inhibitory activity of Cdk p21. Its activity leads to phosphorylation of the retinoblastoma protein (pRb) and promotes tumor cell growth and proliferation. STRAP has both oncogenic and suppressive potential, depending on the tissue type. Its suppressive function has been demonstrated in the colon [44]. STRAP was downregulated in cell lines treated with NTBF OMVs. [44]. Thus, it can be assumed that overexpressed SNN and SERPINB5 may increase cell growth and proliferation, which can generally be supported by the suppressive potential of downregulated STRAP. Together, these proteins may promote cell survival under OMV attack [45].

The most interesting variants of proteins that were up- and downregulated in SW-837 cell lines treated with ETBF OMVs were BRD7, TPM3 and prohibitin. TPM3 is involved in the activation of epithelial–

mesenchymal transition, with subsequent E-cadherin degradation and subsequent cell migration [46]. Interestingly, ETBF OMVs containing fragilysin promoted the enzymatic degradation of E-cadherin. Since E-cadherin is an indirect substrate of fragilysin, TPM3 overexpression can be defined as a concomitant regulatory factor for modifying intercellular adhesion. The BRD7 protein, which was downregulated in the SW837 cell line treated with ETBF OMVs, is a regulator of the Wnt signaling pathway [47]. Its direct interaction with cadherins is necessary for its inhibitory effect on tumor growth. When the BRD7 protein is downregulated, tumor growth is expected to increase. Prohibitin, a global regulator of cell proliferation and apoptosis, was downregulated in cell cultures treated with ETBF-OMVs. The overexpression of prohibitin has been described as one of the possible mechanisms of transformation from adenoma to colorectal cancer. Prohibin is involved in Wnt pathway regulation and contributes to the negative regulation of apoptosis [48]. Thus, cell lines treated with ETBF and NTBF OMVs are able to enhance cell proliferation, contributing to cell survival under bacterial vesicle attack.

A significant increase in previously observed and newly detected proteomic effects was observed in the cell lines treated with ETBF or NTBF OMVs for 5 hours. Only one of the pathways (HSA-446353 or hsa04141) was involved in cell response in each cell line treated with ETBF or NTBF OMVs for 3 hours. However, global proteome changes occurred in the cell lines treated with ETBF or NTBF OMVs for 5 hours. More than 30 different pathways were observed in cell cultures treated with NTBF-OMVs. Interestingly, the most significant signaling pathways included the following upregulated proteins: YWHAB, YWHAQ, and YWHAZ. These proteins are the basis of the cell cycle signaling pathway, infection disease and immunity signaling pathway, cell death signaling pathway, SARS-CoV-1/SARS-CoV-2 infection signaling pathway and transcriptional regulation by the TP53 signaling pathway. This group of proteins is involved in a wide range of protein interactions, mainly affecting cell proliferation and cell apoptosis. It is known that inhibition of these proteins leads to cell apoptosis. For example, the YWHAB protein plays important roles in cancer signaling. Overall, YWHAB, YWHAQ and YWHAZ are considered to be tumor suppressors, and their downregulation has been frequently detected in many types of cancer [49, 50]. Since upregulation of YWHAB was observed in cultures treated with NTBF OMVs, it can be assumed that cells continue to receive an additional proliferative stimulus when in contact with bacterial vesicles. The involvement of proteins that are the basis of the SARS-CoV-1/SARS-CoV-2 infection signaling pathway in the process of cell-bacterial OMV interaction is probably a consequence of the presence of common targets/receptors for viruses and bacterial vesicles on/in epithelial cells. In the virion, SARS-CoV-1 N binds to the host protein YWHAB, which regulates nucleocytoplasmic trafficking [51].

Several signaling pathways associated with these proteins (YWHAB, YWHAQ, and YWHAZ) were also observed in cell lines treated with the ETBF OMV. The associated pathways were as follows: apoptosis (HSA-109581), immune system (HSA-168256), infectious disease (HSA-5663205), negative regulation of NOTCH4 signaling (HSA-9604323), signaling by Rho GTPases (HSA-194315) and innate immune system (HSA-168249). The immune system (HSA-168256) and innate immune system (HSA-168249) pathways observed in cell line treated by ETBF OMVs deserve more attention because overexpressed Serpin B3, which is involved in the regulation of the abovementioned pathways, modulates the host immune

response against tumor cells and promotes cell apoptosis. Dysregulation of SerpinB3, COX-2 and β-catenin has been shown to be associated with more advanced tumor stages in colorectal cancer patients. The in vitro results supported a driving role of SerpinB3 in the upregulation of the COX-2/β-catenin positive loop, which is associated with a more aggressive cellular phenotype [52]. Previously, *Bacteroides fragilis* toxin was shown to coordinate a pro-carcinogenic inflammatory pathway by targeting colonic epithelial cells [53]. SerpinB3 likely plays a key role in the formation of complex tumorigenic reactions in cells treated with ETBF OMVs. Fragilysin associated with ETBF OMVs can possibly contribute to the overexpression of SerpinB3 and further promote the activation of the MAPK6/MAPK4 signaling pathway (HSA-5687128) [54].

IL18 is a proinflammatory cytokine primarily involved in epithelial barrier repair, polarized T helper 1 (Th1) cell and natural killer (NK) cell immune responses [55]. IL18 was found to be overexpressed in cell lines treated with NTBF OMVs. The secretion of a proinflammatory cytokine is particularly surprising, as the expected effect of NTBF OMVs is to reduce the inflammatory response. However, *B. fragilis* capsular polysaccharide A (PSA) is associated with OMVs and is delivered to intestinal dendritic cells (DCs) to induce interleukin-10 (IL-10) production. IL10 suppresses inflammation [42]. It is possible that IL-18 may play a profound role during the initiation phase of an immune response by recruiting plasmacytoid DCs and modulating the function of DC2s [56]. The recruited DCs further interact with PSA-containing OMVs. A possible mechanism of the suppression of epithelial cell inflammation by the secretion of IL18 is shown in Fig. 7.

Increased amounts of FLNA and HSPB1 were observed in the cultures treated with EBTF OMVs. Both proteins are involved in the pathway involving interleukin-18. However, in cell lines treated with ETBF OMVs, the upregulation of HSPB1 did not lead to the secretion of interleukin-18, as observed in the culture treated with NTBF OMVs. However, it can be assumed that similar mechanisms may also be active in cell culture when treated with ETBF OMVs. The main problem with a timely anti-inflammatory response is probably related to the presence of a toxin that can delay such effects by affecting the cell cytoskeleton. We hypothesized that the cytoskeleton structure of cells treated with the toxin rebuilds and is therefore unable to respond to OMV attack in a timely manner. This hypothesis and the mechanism underlying the IL18-mediated suppression of inflammation require further experimental evaluation.

CONCLUSION

In this study, a comparative proteomic analysis of SW-837 cell cultures treated with ETBF and NTBF OMVs identified dysregulated proteins involved in multiple signaling pathways supporting mainly cell proliferation. A significantly greater number of proteomic effects were observed in cell lines treated with NTBF OMVs than in those treated with ETBF OMVs containing toxins. Fragilysin may delay the proliferative effects of ETBF OMVs on cell lines by affecting the cell cytoskeleton which will be confirmed in subsequent experiments. IL-18 secretion has been observed in cell lines treated with NTBF OMVs. IL18 contributes to the initiation of an immune response by recruiting plasmacytoid DCs, which then interact with PSA located on the surface of OMVs to suppress inflammation. It is important to note that

ETBF and NTBF OMVs contain various enzymes that determine the combined molecular effect of different types of vesicles. It is important to note that vesicles contain various enzymes that determine the overall molecular effect, and further study of the influence of individual components can determine the formation of new aspects of the proinflammatory and antitumor pathways activation.

MATERIALS AND METHODS

Bacterial strains and cell cultures

Enteropathogenic *Bacteroides fragilis* (ETBF) (*B. fragilis* strain BOB25) and non-toxigenic *B. fragilis* 323-J-86 (clinical isolates kindly provided from the Federal Research and Clinical Centre of Physical-Chemical Medicine Federal Medical Biological Agency, Moscow, Russia) were grown on blood agar plates containing either 5% defibrinated horse blood or brain heart infusion broth supplemented with hemin (5 g/ml) under anaerobic conditions. The bacterial cultivation was maintained until the mid-logarithmic phase, corresponding to an optical density of 0.7 [9].

Human colonic epithelial cells (HT-29 and SW837) were obtained from the American Type Culture Collection (ATCC Number HTB-38 and ATCC Number CCL-235). Both cell lines were cultured under similar conditions. The cells were scattered into culture flasks (25 cm2) in DMEM (Life Technologies, USA) supplemented with 10% fetal calf serum (Gibco, USA), 2 mM GlutaMax (Life Technologies, USA), and 50 µg/ml gentamicin (Life Technologies, USA) and incubated at 37°C in an atmosphere of 5% CO2.

OMV isolation

The overnight *B. fragilis* culture (200 ml) was centrifuged at 4500 × g at 4°C. The supernatant was collected and further filtered through a 0.45 µm pore size filter (Millex GV; Millipore). The supernatant obtained after filtration was subjected to ultracentrifugation at 100,000 × g for 1,5 hours (Optima L-90K ultracentrifuge; Beckman Coulter). The precipitate obtained by ultracentrifugation was resuspended in sterile phosphate-buffered saline (PBS) and additionally filtered through filters with a polyvinylidene fluoride membrane with a pore diameter of 0.22 µm (Millex GV; Millipore). The resulting filtrate was ultracentrifuged again. The sediment was resuspended in 150 mM NaCl (pH 6.5). Forty micrograms of each OMV sample (NTBF and ETBF) were mixed with Laemmli sample buffer and separated by SDS–PAGE to visually characterize the OMV proteins. The isolated OMVs, prepared for cell culture experiments, were resuspended and then stored in a freezer at -80°C. They were subjected to a single thawing before use, with their structural integrity confirmed in our previous studies through transmission electron microscopy.

TEM and NTA

For TEM, the vesicles were resuspended in phosphate-buffered saline (5 µl) and negatively counterstained with 2% uranyl acetate for 3 minutes. The resulting preparations were examined by electron microscopy using a Zeiss Libra 120 electron microscope (Zeiss, Germany) at a magnification of 10,000 to 40,000. The NTA method was used for OMV concentration and size measurements. The

procedure for determining the concentration and size of OMVs using the NTA method is described in [21].

Epithelial cell lines and isolated OMVs coincubation

The cell lines (HT-29 and SW837) were seeded in a six-well culture plate (1 million cells per well) and incubated in serum-containing medium until the monolayer reached 80% confluence. The serum-containing medium was then replaced with serum-free DMEM by washing the culture three times with phosphate-buffered saline. The ETBF and NTBF OMVs obtained by centrifugation were added to the wells in 3 technical replicates at a concentration of 5×10^13 particles/ml. Cultures and OMVs were coincubated at 37°C in a 5% CO2 atmosphere for three or five hours. The cells were then washed three times with phosphate-buffered saline and collected with a rubber scrubber in a volume of 1 ml of buffer solution. The cells were washed three times by centrifugation at 300 × g for 15 minutes. The resulting cell pellet was frozen at -200°C. The experiment was performed with 3 biological replicates.

Cell viability assay

The cell viability assay was performed 5 hours after the OMVs were added to the cells. A commercially available LIVE/DEAD viability/cytotoxicity kit (Life Technologies, USA) was used. After incubation with OMVs, the cells were washed three times with phosphate-buffered saline and stained with Hanks' solution containing calcein AM and ethidium homodimer-1 (both at a concentration of 2.5 µM for 20 minutes at 37°C). After staining, the cells were immediately observed under an epifluorescence microscope. Micrographs were taken from ten randomly selected fields of view (20x objective, linear field dimensions: 440 µm × 331 µm). Live and dead cells were counted visually.

Western blot hybridization

ETBF and NTBF OMVs were added to culture plates containing SW 837 cells for 15 min and 2 hours. After incubation, the cells were washed with phosphate-buffered saline, mixed with Laemmli buffer containing CHAPS at a ratio of 1:1 and incubated at 95°C. Forty micrograms of protein isolated from cell samples was subjected to electrophoretic separation via SDS—PAGE, followed by Western blot analysis. After electrophoresis, proteins were transferred semidry to a PVDF membrane (Amersham Biosciences, USA) at 1 mA per cm2 of gel for 2 hours. The membrane was incubated for 30 minutes in 1x PBS with 5% milk (Bio-Rad, USA) and then overnight at 4°C with primary antibodies against E-cadherin (Amersham Biosciences, USA) diluted in 1x PBS with 5% milk (1:1000). The membrane was washed 3 times for 10 minutes in 1x phosphate-buffered saline (PBS). The membrane was incubated with a secondary antibody for 1 hour at room temperature. The secondary antibody used was donkey anti-rabbit immunoglobulin G conjugated to horseradish peroxidase (Amersham Biosciences, USA) at a dilution of 1:50,000. The membrane was washed three times for 10 minutes in PBS. The ECL Plus Kit (Amersham Biosciences, USA) was developed according to the manufacturer's instructions. The signal was detected using a ChemiDoc MP gel documentation system (Bio-Rad, USA).

Two-dimensional gel electrophoresis

Prior to two-dimensional electrophoresis, 5 µl of detergent mixture (30% CHAPS and 10% NP 40) and 1 µl of nuclease mixture (Nuclease Mix, GE Healthcare) were added to the cell sediment and incubated at 4°C for 30 min. The proteins were then reprecipitated with methanol/chloroform and dissolved in isoelectric focusing buffer (40 mM Tris-HCl, pH 9.5, containing 8 M urea, 2 M thiourea, and 4% CHAPS + NP40). The samples were centrifuged at 14,000 × g for 15 minutes. After centrifugation, the supernatant was collected, and the protein concentration was measured by the Bradford method using the Quick Start Bradford dye reagent (Bio-Rad). Proteins were then labeled with CyDye3-DIGE (green fluorescence) and CyDye5-DIGE (red fluorescence) according to the manufacturer's recommendations (Amersham). After 45 min, the cyanine-protein binding reaction was stopped with a 10 mM lysine solution, DTT was added to a final concentration of 100 mM, and ampholytes 3–10 to 1% were added. Prior to the mixing stage of the two samples to be compared, electrophoretic separation of each sample was performed by 12% PAGE under denaturing conditions. After electrophoresis, the gel was scanned on a TyphoonTrio scanner (Amersham) at laser wavelengths of 532 nm (green fluorescence) and 633 nm (red fluorescence), and the total fluorescence intensity for each sample was determined. Taking these values into account, two samples labeled with different cyanines were mixed at a certain ratio, taking into account the equalization of the total fluorescence intensity values for each of them. Isoelectric focusing was performed in 18 cm glass tubes in 4% PAAG containing 8 M urea, 2% ampholine (pH 3–10), 4% ampholine (pH 5–8), a 6% mixture of two detergents (30% CHAPS and 10% NP 40), 0.1% TEMED, and 0.02% ammonium persulfate. Total protein (200 µg) was added to the tubes. Isoelectric focusing was performed in the following modes: 100 V – 200 V – 300 V – 400 V – 500 V – 600 V – 45 minutes each, 700 V – 10 hours, and 900 V – 1 hour. After completion of isoelectric focusing, the tubes were equilibrated for 30 minutes in buffer containing 6 M urea, 30% glycerol, 62.5 mM Tris-HCl (pH 6.8), 2% sodium dodecyl sulfate, 20 mM DTT, and bromophenol blue. The tubes were then transferred to the surface of a gradient polyacrylamide gel (9–16%) and fixed with 0.9% bromophenol blue agarose. Electrophoresis was performed in Tris-glycine buffer in the following mode: 20 mA per glass for 20 minutes, 40 mA per glass for 2 hours, and 35 mA per glass for 2.5 hours with the chamber cooled to 100°C. The resulting gels were scanned on a TyphoonTrio scanner (Amersham) at laser wavelengths of 532 nm (green fluorescence) and 633 nm (red fluorescence). The gel images were processed using PDQuest software (Bio-Rad). Silver staining was performed as described by Shevchenko A [23]. Tryptic hydrolysis of proteins was performed as described by Zgoda V [24].

Mass spectrometry and data identification

The mass spectrometry preparation protocol was adapted from Ref. Zgoda V [24]. Mass spectra were obtained on an Ultraflex II BRUKER tandem MALDI time-of-flight mass spectrometer (Germany) equipped with a UV laser (Nd). Mass spectra were obtained in positive ion mode using a reflector; the accuracy of the measured masses after calibration with trypsin autolysis peaks was 0.007%, and the accuracy of the measured fragment masses was 1 Da. Protein identification was performed using Mascot (www.matrixscience.com). A "peptide fingerprint" search was performed in the NCBI database among proteins with the specified accuracy, taking into account the possible oxidation of methionine by atmospheric oxygen and the possible modification of cysteines by acrylamide.

RT-PCR

Total RNA was isolated using QIAGEN RNeasy Plus universal kits (Qiagen, Germany) according to the manufacturer's instructions. Quantitative real-time polymerase chain reaction (qRT-PCR) was performed using the Bio-Rad CFX 96 Real-Time Detection System (Bio-Rad, USA). Oligonucleotide primers and amplification conditions are listed in **Supplementary table S8**. qPCRmix-HS-SYBR (Evrogen, Russia) was used to prepare reaction mixtures. The specificity of the reaction products was confirmed by melting point analysis (from 70°C to 95°C in 0.5°C/15 s steps). The level of GAPDH mRNA was used to normalize the expression ratio of the genes of interest. All reactions were performed three times, and the final analysis was based on the average value of the reactions. The relative quantification method 2-ΔΔct was used in further calculations.

Proteome data analysis

Pathways were constructed with the following resources: the STRING database (https://string-db.org/), https://www.genecards.org/, and https://www.genome.jp/. The STRING database estimates the probability of protein interactions in pairs based on data from available databases. When calculating the probability of interaction, the similarity of amino acid sequences, protein functions and other aspects are taken into account. FDR was used for multiple comparison correction.

Declarations

Ethics Approval and Consent to Participate

Not applicable.

Consent for Publication

Not applicable.

Author contributions

O.Y.S., D.A.K., O.V.P., and N.B.Z. designed and performed the experiments, analyzed the data and wrote the paper; D.A.K., D.S.M., B.A.E., A.S.S., A.V.C, A.V.C, I.V.P., I.V.K., V.D.K. and A.A.V. performed the experiments; E.A.V. analyzed the data; and N.B.Z. supervised the project.

Data availability

The data that support the findings of this study are openly available in ProteomeXchange at https://www.ebi.ac.uk/pride/, reference number PXD060818.

Funding support

This research was supported by RSF grant 24-75-10100

Conflict of interest

No, there is no conflict of interest

Acknowledgments

The TEM measurements were carried out at the User Facilities Center “Electron microscopy in life sciences” of Lomonosov Moscow State University. We thank Mr. Alexey Senkovenko and Mr. Dmitry V. Bagrov for the assistance with TEM imaging. We thank Mr. Evgeniy G. Evtushenko for the assistance with NTA.

Additional information

A preprint has previously been published: https://www.researchsquare.com/article/rs-3970402/v1 [58]

References

1. Sommer F, Bäckhed F (2013) The gut microbiota–masters of host development and physiology. Nat Rev Microbiol 11(4):227–238. 10.1038/nrmicro2974. Epub 2013 Feb 25. PMID: 23435359
2. Coyne MJ, Roelofs KG, Comstock LE, Coyne MJ, Roelofs KG, Comstock LE (2016) Type VI secretion systems of human gut Bacteroidales segregate into three genetic architectures, two of which are contained on mobile genetic elements. *BMC Genomics.* 17 (1) C.58
3. Salyers AA (1984) Bacteroides of the Human Lower Intestinal Tract. Annu Rev Microbiol 38(1):–293
4. Wexler HM (2007) Bacteroides: the good, the bad, and the nitty-gritty. *Clinical microbiology reviews*. 20 (4) C.593–621
5. Hooper LV, Midtvedt T, Gordon JI (2002) How host–microbe interactions shape the nutrient environment of the mammalian intestine. *Annual Review of Nutrition* 22 (1): C.283–307
6. Reeves AR, D’Elia JN, Frias J, Salyers AA (1996) A Bacteroides thetaiotaomicron outer membrane protein that is essential for utilization of maltooligosaccharides and starch. *Journal of bacteriology.* 178 (3) C.823–30
7. Shin JH, Tillotson G, MacKenzie TN, Warren CA, Wexler HM, Goldstein EJC (2024) Bacteroides and related species: The keystone taxa of the human gut microbiota. Anaerobe 85:102819. 10.1016/j.anaerobe.2024.102819. Epub ahead of print. PMID: 38215933
8. Wu S, Rhee K-J, Zhang M, Franco A, Sears CL (2007) *Bacteroides fragilis* toxin stimulates intestinal epithelial cell shedding and -secretase-dependent E-cadherin cleavage. *Journal of Cell Science*. 120. (20): C.3713–3713
9. Zakharzhevskaya NB, Vanyushkina AA, Altukhov IA, Shavarda AL, Butenko IO, Rakitina DV, Nikitina AS, Manolov AI, Egorova AN, Kulikov EE, Vishnyakov IE, Fisunov GY, Govorun VM (2017) Outer membrane vesicles secreted by pathogenic and nonpathogenic *Bacteroides fragilis* represent different metabolic activities. Sci Rep 7(1):5008. 10.1038/s41598-017-05264-6. PMID: 28694488; PMCID: PMC5503946

10. Wu S *Bacteroides fragilis* Enterotoxin Induces c-Myc Expression and Cellular Proliferation/Wu S., Morin P.J., Maouyo D., Sears C.L
11. Saidi RF, Sears CL (1996) *Bacteroides fragilis* toxin rapidly intoxicates human intestinal epithelial cells (HT29/C1) in vitro. *Infection and immunity*. 64 (12): C.5029–34
12. Kharlampieva DD, Manuvera VA, Podgorny OV, Kovalchuk SI, Pobeguts OV, Altukhov IA, Alexeev DG, Lazarev VN, Govorun VM (2013) Purification and characterization of recombinant *Bacteroides fragilis* toxin-2. Biochimie 95(11):2123–2131 Epub 2013 Aug 15. PMID: 23954621
13. Purcell RV, Pearson J, Aitchison A, Dixon L, Frizelle FA, Keenan J (2017) I.Colonization with enterotoxigenic *Bacteroides fragilis* is associated with early-stage colorectal neoplasia. PLoS ONE 12(2):–e0171602
14. Wu S, Rhee K-J, Albesiano E, Rabizadeh S, Wu X, Yen H-R, Huso DL, Brancati FL, Wick E, McAllister F, Housseau F, Pardoll DM (2009) Sears C.L. A human colonic commensal promotes colon tumorigenesis via activation of T helper type 17 T-cell responses. *Nature medicine.* 15 (9) C.1016–22
15. Mazmanian SK (2008) Capsular polysaccharides of symbiotic bacteria modulate immune responses during experimental colitis. J Pediatr Gastroenterol Nutr. 46. Suppl 1 – № Suppl 1 – C.E11-2.
16. Telesford KM, Yan W, Ochoa-Reparaz J, Pant A, Kircher C, Christy MA, Begum-Haque S, Kasper DL (2015) Kasper L.H. A commensal symbiotic factor derived from *Bacteroides fragilis* promotes human CD39(+) Foxp3(+) T cells and Treg function. *Gut microbes*. 6 (4) C.234–42
17. Filloux A (2011) Protein Secretion Systems in *Pseudomonas aeruginosa*: An Essay on Diversity, Evolution, and Function. Front Microbiol. 2. C.155.
18. Elhenawy W, Debelyy MO, Feldman MF (2014) Preferential Packing of Acidic Glycosidases and Proteases into Bacteroides Outer Membrane Vesicles. *mBio*. 5 (2). C.e00909-14-e00909-14
19. Beveridge TJ (1999) Structures of gram-negative cell walls and their derived membrane vesicles. *Journal of bacteriology*. 181 (16). C.4725–33
20. ELee E-Y, Bang JY, Park GW, Choi D-S, Kang JS, Kim H-J, Park K-S, Lee J-O, Kim Y-K, Kwon K-H, Kim K-P (2007) Gho Y.S. Global proteomic profiling of native outer membrane vesicles derived fromEscherichia coli. *PROTEOMICS*. 7(17). C.3143–3153
21. Shagaleeva OY, Kashatnikova DA, Kardonsky DA, Konanov DN, Efimov BA, Bagrov DV, Evtushenko EG, Chaplin AV, Silantiev AS, Filatova JV, Kolesnikova IV, Vanyushkina AA, Stimpson J, Zakharzhevskaya NB (2023) Investigating volatile compounds in the Bacteroides secretome. Front Microbiol 14:1164877 PMID: 37206326; PMCID: PMC10189065
22. Shen Y, Giardino Torchia ML, Lawson GW, Karp CL, Ashwell JD, Mazmanian SK (2012) Outer membrane vesicles of a human commensal mediate immune regulation and disease protection. *Cell host & microbe*. 12 (4). C.509–20
23. Shevchenko A, Wilm M, Vorm O, Mann M (1996) Mass spectrometric sequencing of proteins silver-stained polyacrylamide gels. *Anal Chem.* ;68(5):850-8. 10.1021/ac950914h. PMID: 8779443

24. Zgoda V, Tikhonova O, Viglinskaya A, Serebriakova M, Lisitsa A, Archakov A (2006) Proteomic profiles of induced hepatotoxicity at the subcellular level. Proteomics 6(16):4662–4670. 10.1002/pmic.200600342
25. Kharlampieva D, Manuvera V, Podgorny O, Grafskaia E, Kovalchuk S, Pobeguts O, Altukhov I, Govorun V, Lazarev V (2015 Jun-Jul) Recombinant fragilysin isoforms cause E-cadherin cleavage of intact cells and do not cleave isolated E-cadherin. Microb Pathog 83–84:47–56 Epub 2015 May 18. PMID: 25998017
26. Larabi A, Barnich N, Nguyen HTT (2020) New insights into the interplay between autophagy, gut microbiota and inflammatory responses in IBD. Autophagy 16(1):38–51. 10.1080/15548627.2019.1635384. Epub 2019 Jul 9. PMID: 31286804; PMCID: PMC6984609
27. Park KS, Svennerholm K, Crescitelli R, Lässer C, Gribonika I, Lötvall J (2021) Synthetic bacterial vesicles combined with tumor extracellular vesicles as cancer immunotherapy. *J Extracell Vesicles.* ;10(9): e12120. 10.1002/jev2.12120. Epub 2021 Jul 3. PMID: 34262675; PMCID: PMC8254025
28. Li A, Schertzer JW, Yong X (2019) Molecular conformation affects the interaction of the Pseudomonas quinolone signal with the bacterial outer membrane. J Biol Chem 294(4):1089–1094. 10.1074/jbc.AC118.006844. Epub 2018 Dec 18. PMID: 30563840; PMCID: PMC6349108
29. Zakharzhevskaya NB, Tsvetkov VB, Vanyushkina AA, Varizhuk AM, Rakitina DV, Podgorsky VV, Vishnyakov IE, Kharlampieva DD, Manuvera VA, Lisitsyn FV, Gushina EA, Lazarev VN, Govorun VM (2017) Interaction of *Bacteroides fragilis* Toxin with Outer Membrane Vesicles Reveals New Mechanism of Its Secretion and Delivery. *Front Cell Infect Microbiol.* ; 7:2. 10.3389/fcimb.2017.00002. Erratum in: Front Cell Infect Microbiol. 2017; 7:308. PMID: 28144586; PMCID: PMC5240029
30. Zhu H, Fang X, Zhang D, Wu W, Shao M, Wang L, Gu J (2016) Membrane-bound heat shock proteins facilitate the uptake of dying cells and cross-presentation of cellular antigen. *Apoptosis*. ;21(1):96–109. 10.1007/s10495-015-1187-0. PMID: 26481477
31. Luis AS, Hansson GC (2023) Intestinal mucus and their glycans: A habitat for thriving microbiota. Cell Host Microbe 31(7):1087–1100. 10.1016/j.chom.2023.05.026. PMID: 37442097; PMCID: PMC10348403
32. Karthikeyan R, Gayathri P, Ramasamy S, Suvekbala V, Jagannadham MV, Rajendhran J (2023) Transcriptome responses of intestinal epithelial cells induced by membrane vesicles of Listeriamonocytogenes. Curr Res Microb Sci 4:100185. 10.1016/j.crmicr.2023.100185. PMID: 36942003; PMCID: PMC10023947
33. Ong MS, Deng S, Halim CE, Cai W, Tan TZ, Huang RY, Sethi G, Hooi SC, Kumar AP, Yap CT (2020) Cytoskeletal Proteins in Cancer and Intracellular Stress. Therapeutic Perspective Cancers (Basel) 12(1):238. 10.3390/cancers12010238. PMID: 31963677; PMCID: PMC7017214
34. Hu C, Yang J, Qi Z, Wu H, Wang B, Zou F, Mei H, Liu J, Wang W, Liu Q (2022) Heat shock proteins: Biological functions, pathological roles, and therapeutic opportunities. MedComm (2020) 3(3):e161. 10.1002/mco2.161. PMID: 35928554; PMCID: PMC9345296

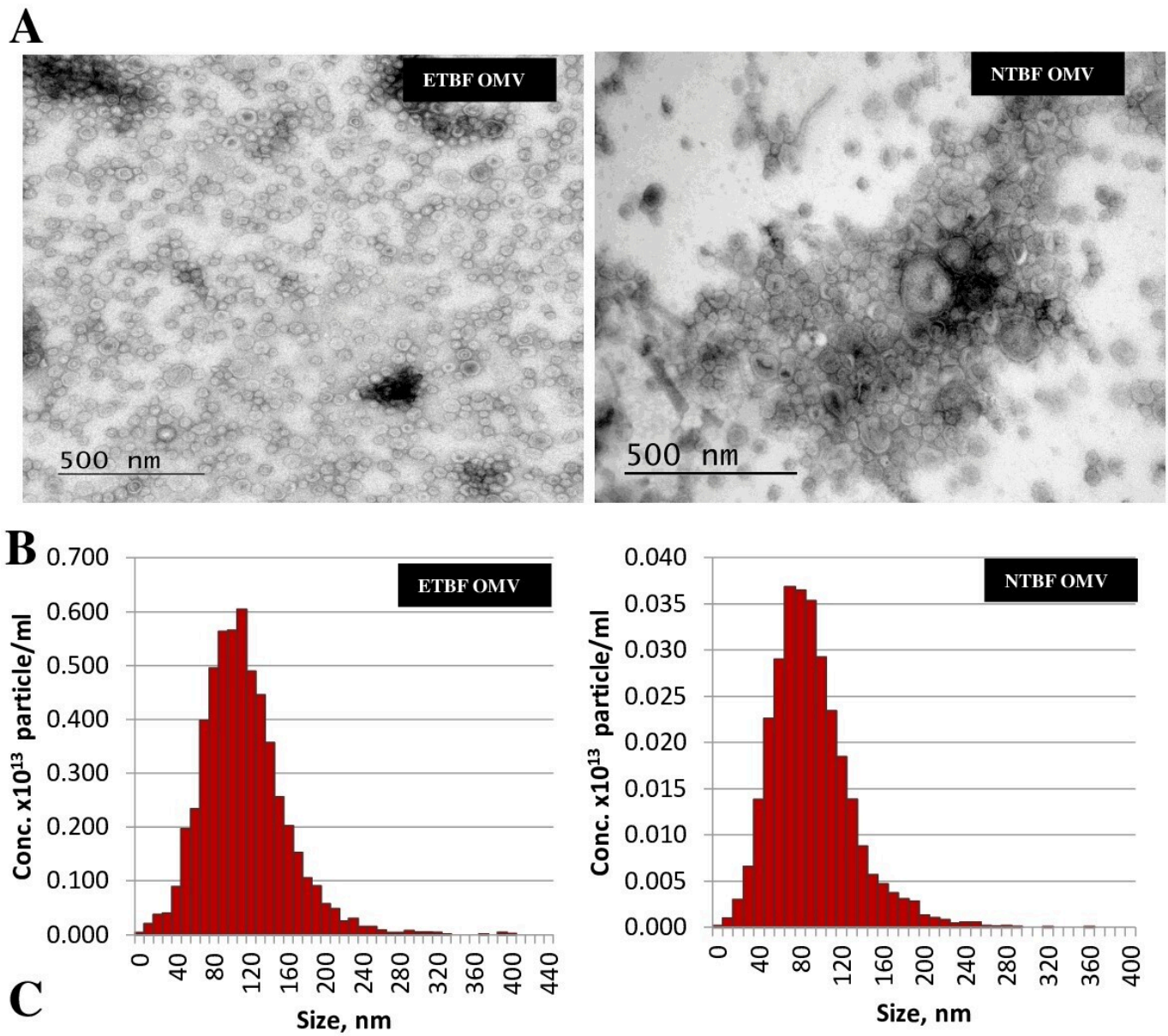
35. Chou RH, Wen HC, Liang WG, Lin SC, Yuan HW, Wu CW, Chang WS (2012) Suppression of the invasion and migration of cancer cells by SERPINB family genes and their derived peptides. Oncol Rep 27(1):238–245. 10.3892/or.2011.1497. Epub 2011 Oct 6. PMID: 21993616
36. Kim JH, Cho NY, Bae JM, Kim KJ, Rhee YY, Lee HS, Kang GH (2015) Nuclear maspin expression correlates with the CpG island methylator phenotype and tumor aggressiveness in colorectal cancer. Int J Clin Exp Pathol 8(2):1920–1928 PMID: 25973084; PMCID: PMC4396253
37. Goley ED, Rammohan A, Znameroski EA, Firat-Karalar EN, Sept D, Welch MD (2010) An actin-filament-binding interface on the Arp2/3 complex is critical for nucleation and branch stability. Proc Natl Acad Sci U S A 107(18):8159–8164. 10.1073/pnas.0911668107. Epub 2010 Apr 19. PMID: 20404198; PMCID: PMC2889539
38. Izdebska M, Zielińska W, Hałas-Wiśniewska M, Grzanka A (2020) Involvement of Actin and Actin-Binding Proteins in Carcinogenesis. Cells 9(10):2245. 10.3390/cells9102245. PMID: 33036298; PMCID: PMC7600575
39. Choi J, Lee YJ, Yoon YJ, Kim CH, Park SJ, Kim SY, Doo Kim N, Cho Han D, Kwon BM (2019) Pimozide suppresses cancer cell migration and tumor metastasis through binding to ARPC2, a subunit of the Arp2/3 complex. Cancer Sci 110(12):3788–3801 Epub 2019 Nov 15. PMID: 31571309; PMCID: PMC6890432
40. Wu YL, Pan LH, Yi ZJ, Zhang WF, Gong JP (2023) c-Myb Dominates TBK1-Mediated Endotoxin Tolerance in Kupffer Cells by Negatively Regulating DTX4. J Immunol Res 2023:5990156. 10.1155/2023/5990156. PMID: 37032653; PMCID: PMC10081914
41. Ogura Y, Bonen DK, Inohara N, Nicolae DL, Chen FF, Ramos R, Britton H, Moran T, Karaliuskas R, Duerr RH, Achkar JP, Brant SR, Bayless TM, Kirschner BS, Hanauer SB, Nuñez G, Cho JH (2001) A frameshift mutation in NOD2 associated with susceptibility to Crohn's disease. *Nature*. ;411(6837):603-6. 10.1038/35079114. PMID: 11385577
42. Chu H, Khosravi A, Kusumawardhani IP, Kwon AH, Vasconcelos AC, Cunha LD, Mayer AE, Shen Y, Wu WL, Kambal A, Targan SR, Xavier RJ, Ernst PB, Green DR, McGovern DP, Virgin HW, Mazmanian SK (2016) Gene-microbiota interactions contribute to the pathogenesis of inflammatory bowel disease. Science 352(6289):1116–1120. 10.1126/science. aad9948. Epub 2016 May 5. PMID: 27230380; PMCID: PMC4996125
43. Davidson CE, Reese BE, Billingsley ML, Yun JK (2005) The protein stannin binds 14-3-3zeta and modulates mitogen-activated protein kinase signaling. *Brain Res Mol Brain Res.* ;138(2):256 – 63. 10.1016/j.molbrainres.2005.04.018. PMID: 15923056
44. Zhang X, Azhar G, Rogers SC, Foster SR, Luo S, Wei JY (2014) Overexpression of p49/STRAP alters cellular cytoskeletal structure and gross anatomy in mice. BMC Cell Biol 15:32. 10.1186/1471-2121-15-32. PMID: 25183317; PMCID: PMC4160719
45. Halder SK, Anumanthan G, Maddula R, Mann J, Chytil A, Gonzalez AL, Washington MK, Moses HL, Beauchamp RD, Datta PK (2006) Oncogenic function of a novel WD-domain protein, STRAP, in

human carcinogenesis. *Cancer Res.* ;66(12):6156-66. 10.1158/0008-5472.CAN-05-3261. PMID: 16778189

46. Choi HS, Yim SH, Xu HD, Jung SH, Shin SH, Hu HJ, Jung CK, Choi JY, Chung YJ (2010) Tropomyosin3 overexpression and a potential link to epithelial–mesenchymal transition in human hepatocellular carcinoma. BMC Cancer 10:122. 10.1186/1471-2407-10-122. PMID: 20356415; PMCID: PMC3087315
47. Chi X, Shan L, Hu Y, Zhang Y, Mao Y, Wang X (2021) Bromodomain-containing protein 7 contributes to myocardial infarction-induced myocardial injury through activating Wnt/β-catenin signaling. *Ann Palliat Med.* ;10(10):10756–10767. 10.21037/apm-21-2433. PMID: 34763437
48. Alula KM, Delgado-Deida Y, Jackson DN, Venuprasad K, Theiss AL (2021) Nuclear partitioning of Prohibitin 1 inhibits Wnt/β-catenin-dependent intestinal tumorigenesis. Oncogene 40(2):369–383. 10.1038/s41388-020-01538-y. Epub 2020 Nov 3. PMID: 33144683; PMCID: PMC7856018
49. Fan X, Cui L, Zeng Y, Song W, Gaur U, Yang M (2019) 14-3-3 Proteins Are on the Crossroads of Cancer, Aging, and Age-Related Neurodegenerative Disease. Int J Mol Sci 20:3518. 10.3390/ijms20143518
50. dXin Z, Chen A (2023) Tingting Zhang YWHAB knockdown inhibits cell proliferation while promoting cell cycle arrest and apoptosis in colon cancer cells through PIK3R2. Exp Ther Med 25(5):193. 10.3892/etm.2023.11892. eCollection 2023 May
51. Kristina V, Tugaeva, Dorothy EDP, Hawkins, Jake LR, Smith OW, Bayfield D-S, Ker AA, Sysoev, Oleg I, Klychnikov AA, Antson (2021) Nikolai N Sluchanko The Mechanism of SARS-CoV-2 Nucleocapsid Protein Recognition by the Human 14-3-3 Proteins. J Mol Biol 433(8):166875. 10.1016/j.jmb.2021.166875. Epub 2021 Feb 5
52. Terrin L, Agostini M, Ruvoletto M, Martini A, Pucciarelli S, Bedin C (2017) Donato Nitti, Patrizia Pontisso SerpinB3 upregulates the Cyclooxygenase-2/β-Catenin positive loop in colorectal cancer. Oncotarget 8(9):15732–15743. 10.18632/oncotarget.14997
53. Chung L, Orberg ET, Geis AL, Chan JL, Fu K, DeStefano Shields CE, Christine M, Dejea P, Fathi J, Chen BB, Finard AJ, Tam F, McAllister H, Wu FX, Ganguly S, Lebid A, Metz P, Sara W, Van Meerbeke DL, Huso EC, Wick, Drew M, Pardoll (2018) Fengyi Wan, Shaoguang Wu, Cynthia L Sears, Franck Housseau *Bacteroides fragilis* Toxin Coordinates a Procarcinogenic Inflammatory Cascade via Targeting of Colonic Epithelial Cells. Cell Host Microbe 23(3):421. 10.1016/j.chom.2018.02.004
54. Wu S, Powell J, Mathioudakis N, Kane S, Fernandez E (2004) Cynthia L Sears *Bacteroides fragilis* enterotoxin induces intestinal epithelial cell secretion of interleukin-8 through mitogen-activated protein kinases and a tyrosine kinase-regulated nuclear factor-kappaB pathway. Infect Immun 72(10):5832–5839. 10.1128/IAI.72.10.5832-5839.2004
55. Kaser A, Kaser S, Kaneider NC, Enrich B, Wiedermann CJ, Tilg H (2004) Interleukin-18 attracts plasmacytoid dendritic cells (DC2s) and promotes Th1 induction by DC2s through IL-18 receptor expression. Blood 103(2):648–655. 10.1182/blood-2002-07-2322. Epub 2003 Sep 22. PMID: 14504095

56. Box JK, Paquet N, Adams MN, Boucher D, Bolderson E, O'Byrne KJ, Richard DJ (2016) Nucleophosmin: from structure and function to disease development. BMC Mol Biol 17(1):19. 10.1186/s12867-016-0073-9. PMID: 27553022; PMCID: PMC4995807
57. Yasuda K, Nakanishi K, Tsutsui H (2019) Interleukin-18 in Health and Disease. Int J Mol Sci 20(3):649. 10.3390/ijms20030649. PMID: 30717382; PMCID: PMC6387150
58. https://www.researchsquare.com/article/rs-3970402/v1

Figures



OMV	Size NTA, nm	Size TEM, nm	Concentration, ×10^13 particles/ml
ETBF	117±4	70±5	5,54±0,60
NTBF	96±3	45±5	0,32±0,04

Figure 1

Electron microscopy of ETBF and NTBF vesicle preparations; (A) Scale bars for ETBF and NTBF are 1 μm; (B) NTA data of ETBF and NTBF OMV concentrations. (C). The NTA data of total particle concentrations of isolated OMVs, ×1013 particles/ml. Error bars represent 95% confidence intervals. Comparative data fordetermining the OMV sizes are given for TEM and NTA.

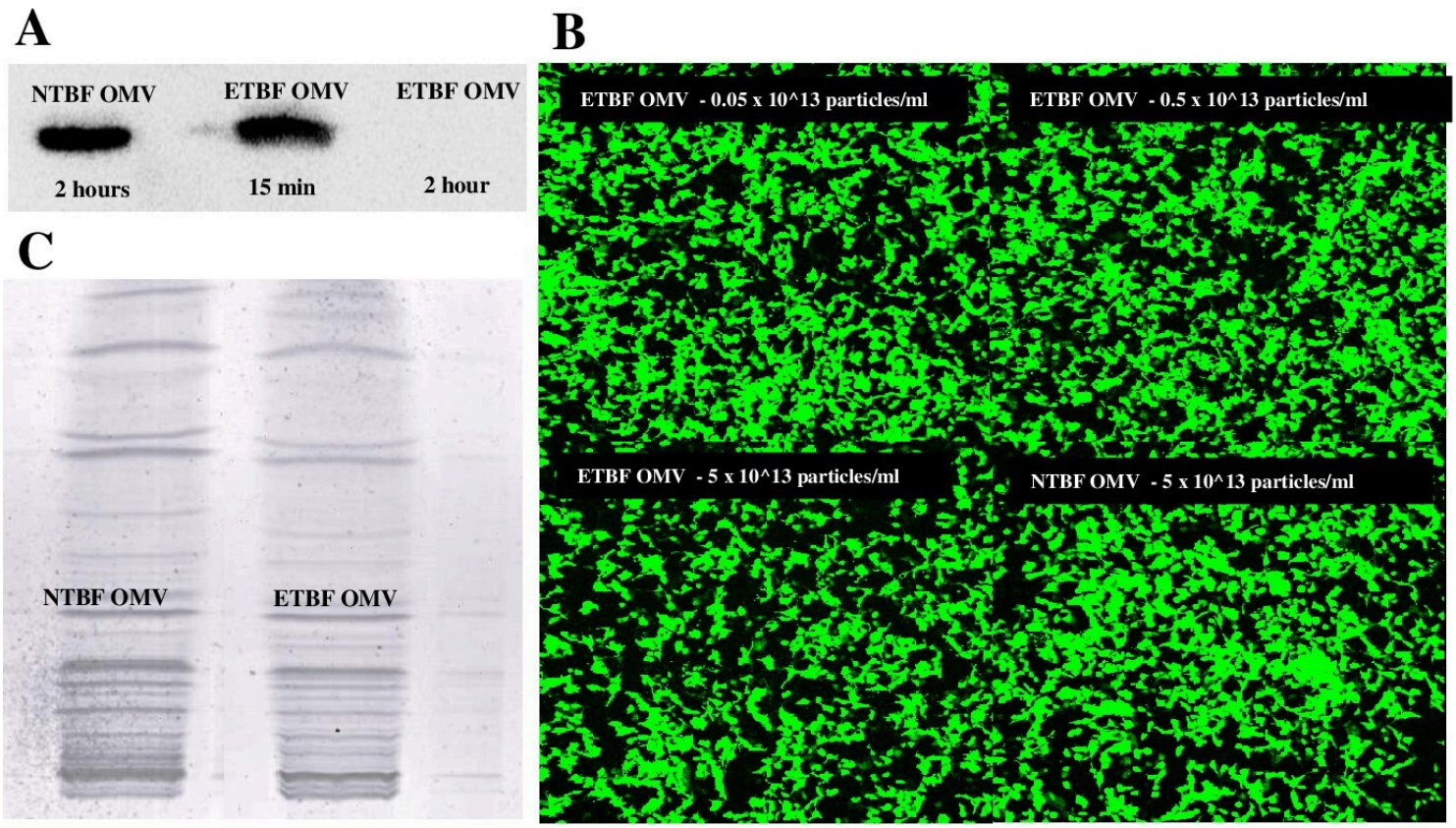


Figure 2

Biological effects of ETBF and NTBF OMVs on E-cadherin in SW837 cell culture. (A) The results of SDS–PAGEseparation of ETBF and NTBF OMVs demonstrated a characteristic spectrum of vesicle proteins. (B) Anti-cadherin antibodies were used to assess the degree of degradation of E-cadherin. The biological effect of vesicle-associated toxins on E-cadherin is time dependent. Fifty micrograms of total protein ETBF OMVs and NTBF OMVs were added to the SW837 cell culture media for 15 minutes and for 2 hours. (C) Fluorescence microscopy of the SW837 cell line exposed to different concentrations of ETBF and NTBF OMVs (0.05 to 5×10^13 particles/ml) with a 10-fold dilution step is shown. The cell viability assay was performed 3 hours after treatment with the OMVs

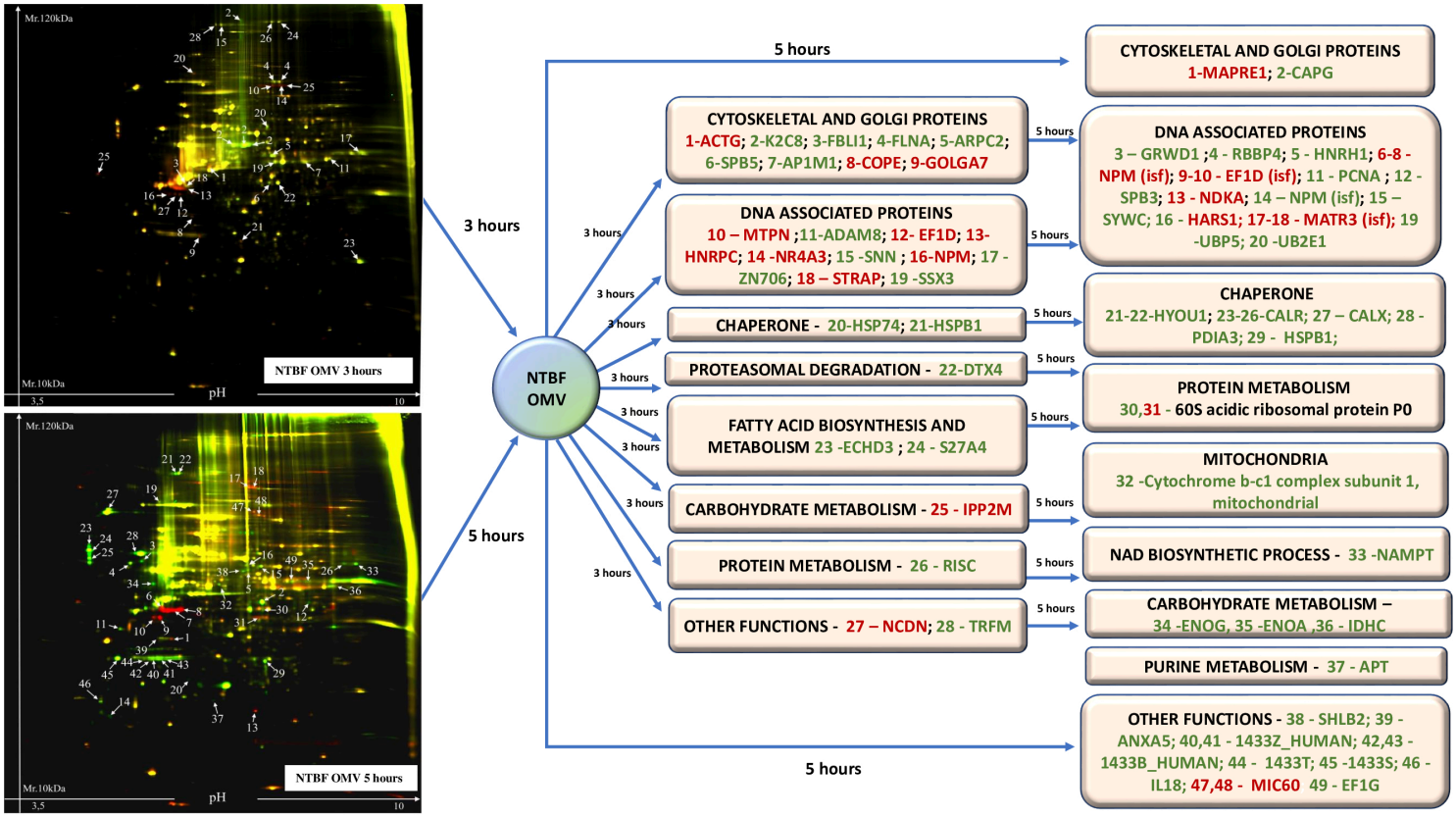


Figure 3

Comparative proteomic analysis of SW837 cell lines treated with NTBF OMVs for 3 and 5 hours was performed by 2D differential gel electrophoresis (pH range 3.5-10). Red fluorophore corresponds to intact cells, and green fluorophore corresponds to cells treated with NTBF-OMVs. The cutoff score for protein identification in the Mascot engine was 44 ($p < 0.05$). The numbers of protein spots indicated by the arrows correspond to the numbers in the boxes. The colors of the proteins in the boxes correspond to the colors in the gels: red indicates downregulated proteins in the cell culture treated with NTBF OMVs, and green indicates upregulated proteins in the cell culture treated with NTBF OMVs.

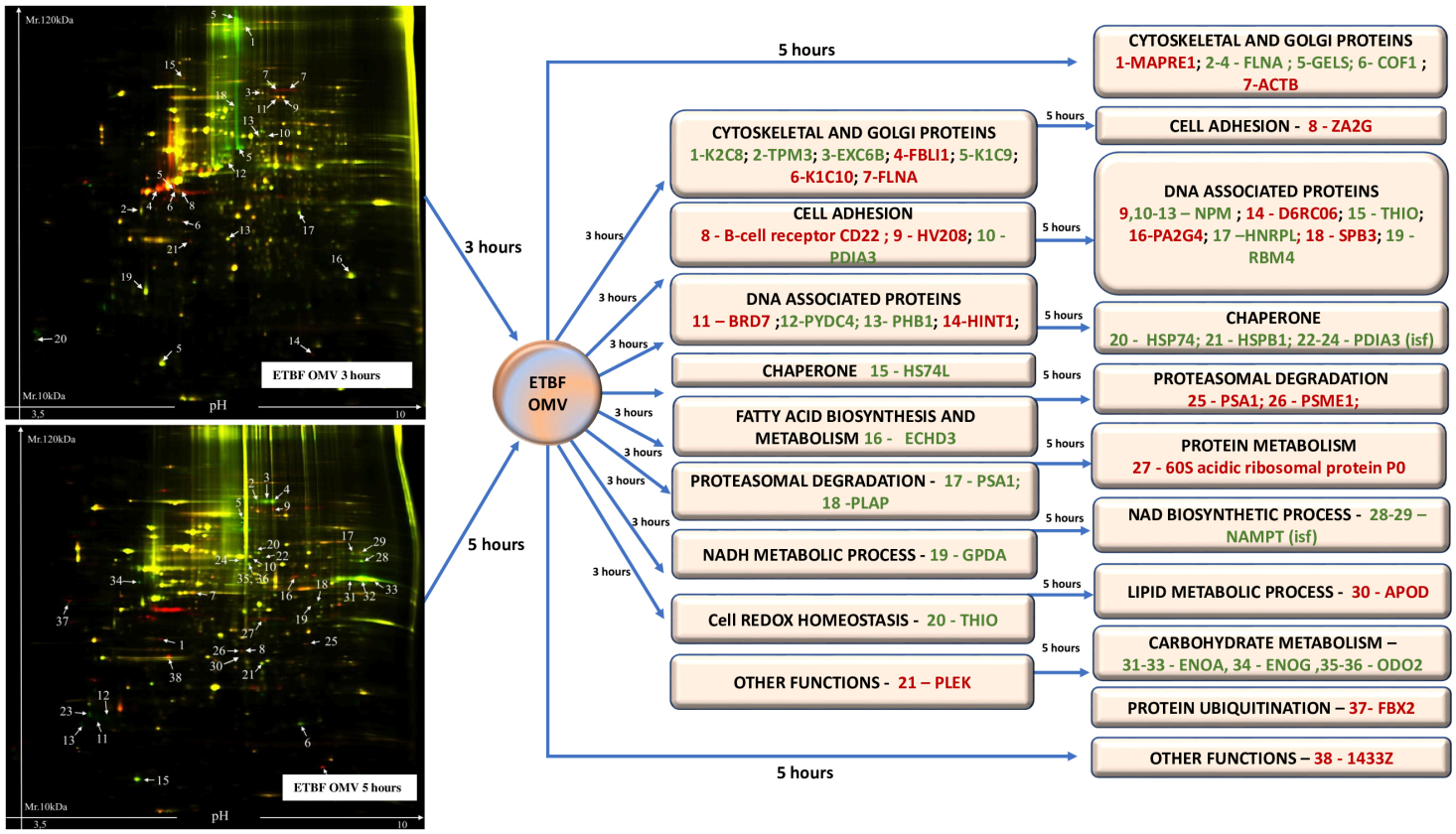


Figure 4

Comparative proteomic analysis of SW837 cell lines treated with ETBF OMVs for 3 and 5 hours was performed by 2D differential gel electrophoresis (pH range 3.5-10). Red fluorophore corresponds to intact cells, and green fluorophore corresponds to cells treated with ETBF-OMVs. The cutoffscore for protein identification in the Mascot engine was 44 ($p < 0.05$). The numbers of protein spots indicated by the arrows correspond to the numbers in the boxes. The colors of the proteins in the boxes correspond to the colors in the gels: red indicates downregulated proteins in the cell culture treated with ETBF OMVs, and green indicates upregulated proteins in the cell culture treated with ETBF OMVs.

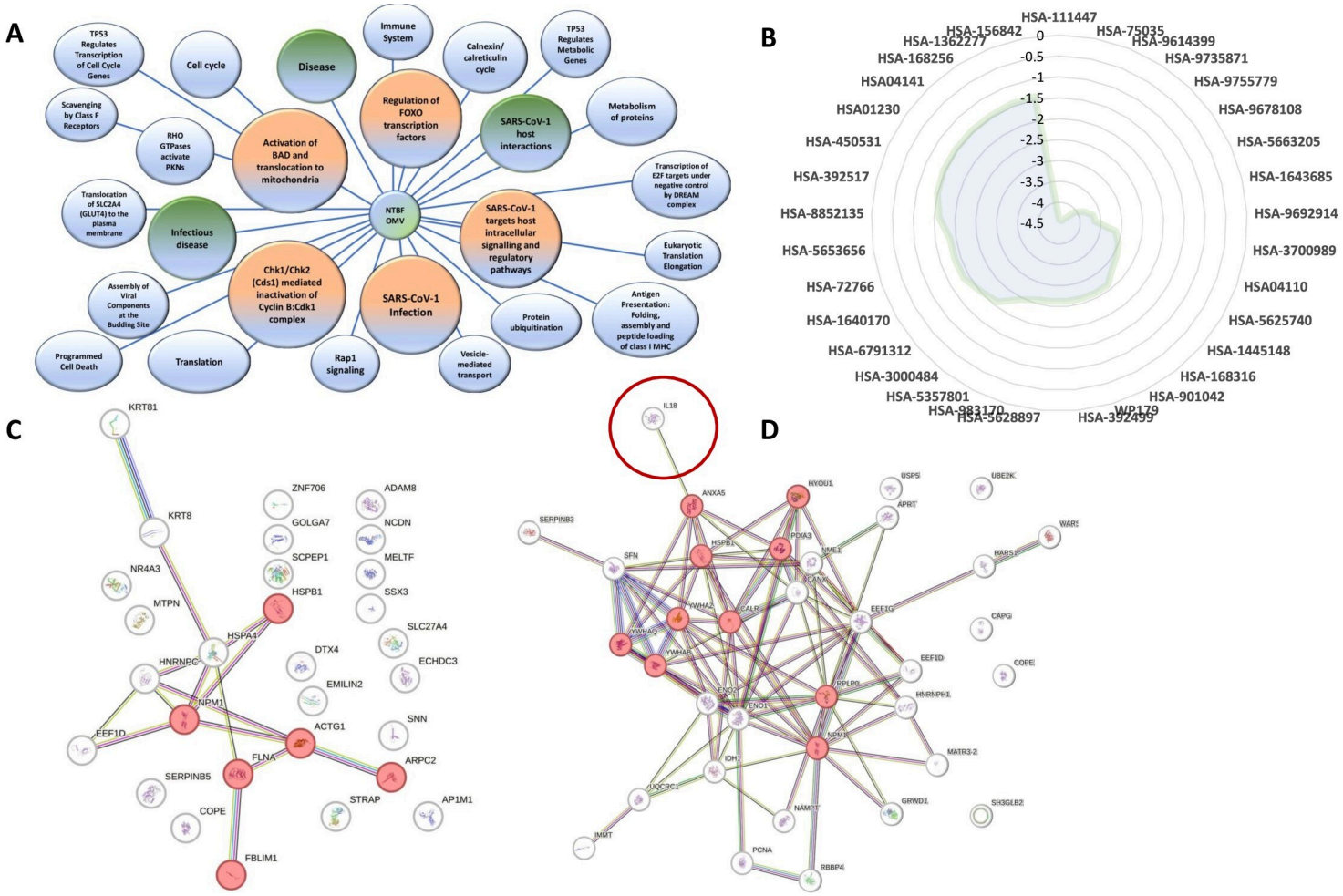


Figure 5

Cell signaling pathways constructed according to the proteomic effects observed in SW-837 cell lines treated with NTBF OMVs. (A) Total data of observed cell signaling pathways in SW-837 cell line culture. The size of the circles correlates with the FDR-adjusted p value. (B) FDR-adjusted p value for all pathways observed in the cell line. Look also **Supplementary table S6** (C) The focal adhesion pathway was observed in cell culture after 3 hours of NTBF OMV exposure. (D) Proteins mapped to signaling pathways observed in cell culture after 5 hours of NTBF-OMVexposure. All the data were analyzed with STRING. https://string-db.org/

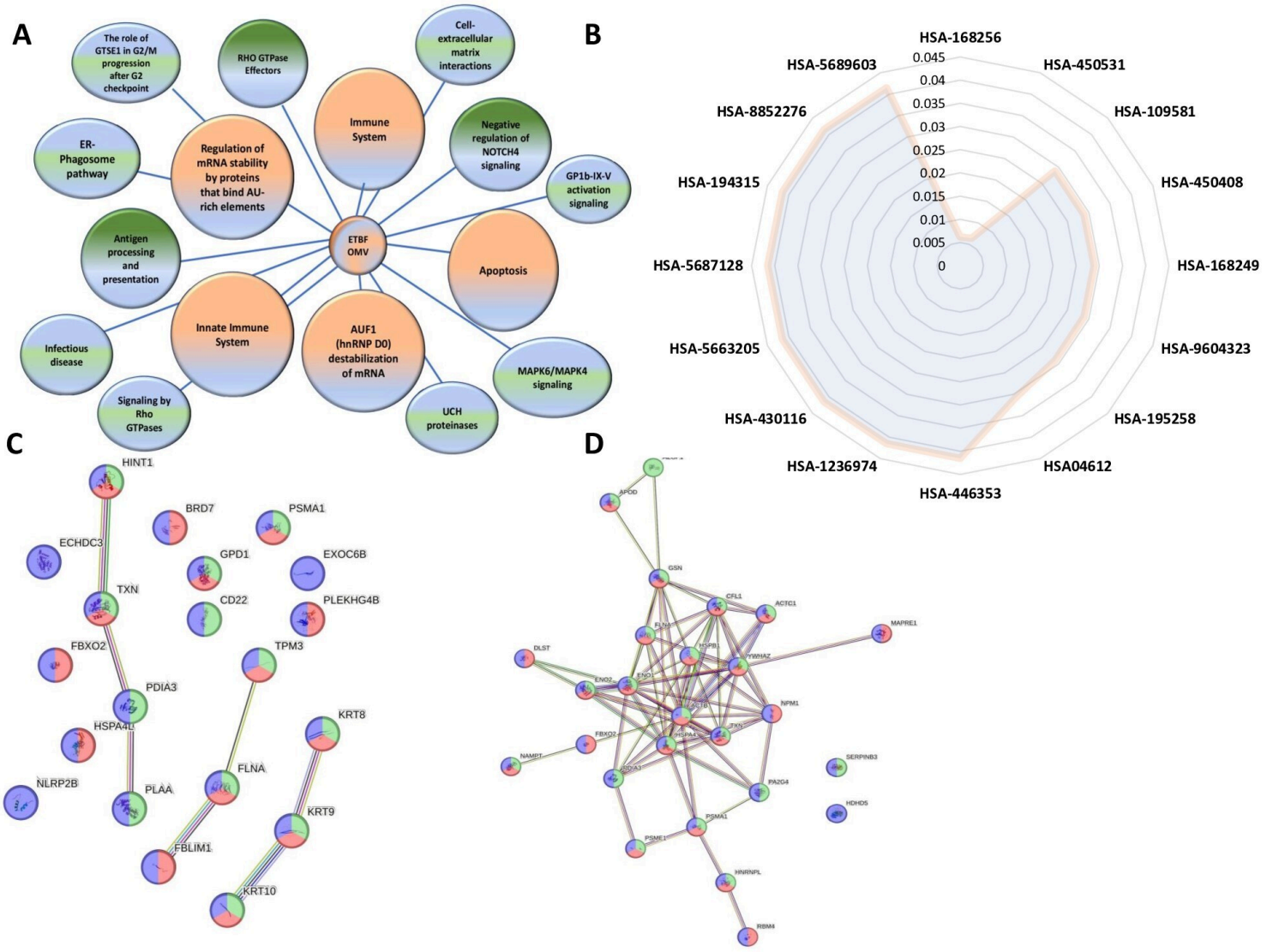


Figure 6

Cell signaling pathways constructed according to the proteomic effects observed in SW-837 cell lines treated with ETBF OMVs. (A) Total data of observed cell signaling pathways in SW-837 cell line culture. The size of the circles correlates with the FDR-adjusted p value. (B) FDR-adjusted p value for all pathways observed in the cell line. Look also **Supplementary table S7** (C) Protein processing in the endoplasmic reticulum pathway was observed in cell culture after 3 hours of ETBF-OMV exposure. (D) Proteins mapped to signaling pathways observed in cell cultures treated with ETBF-OMVs for 5 hours. All the data were analyzed with STRING. https://string-db.org/

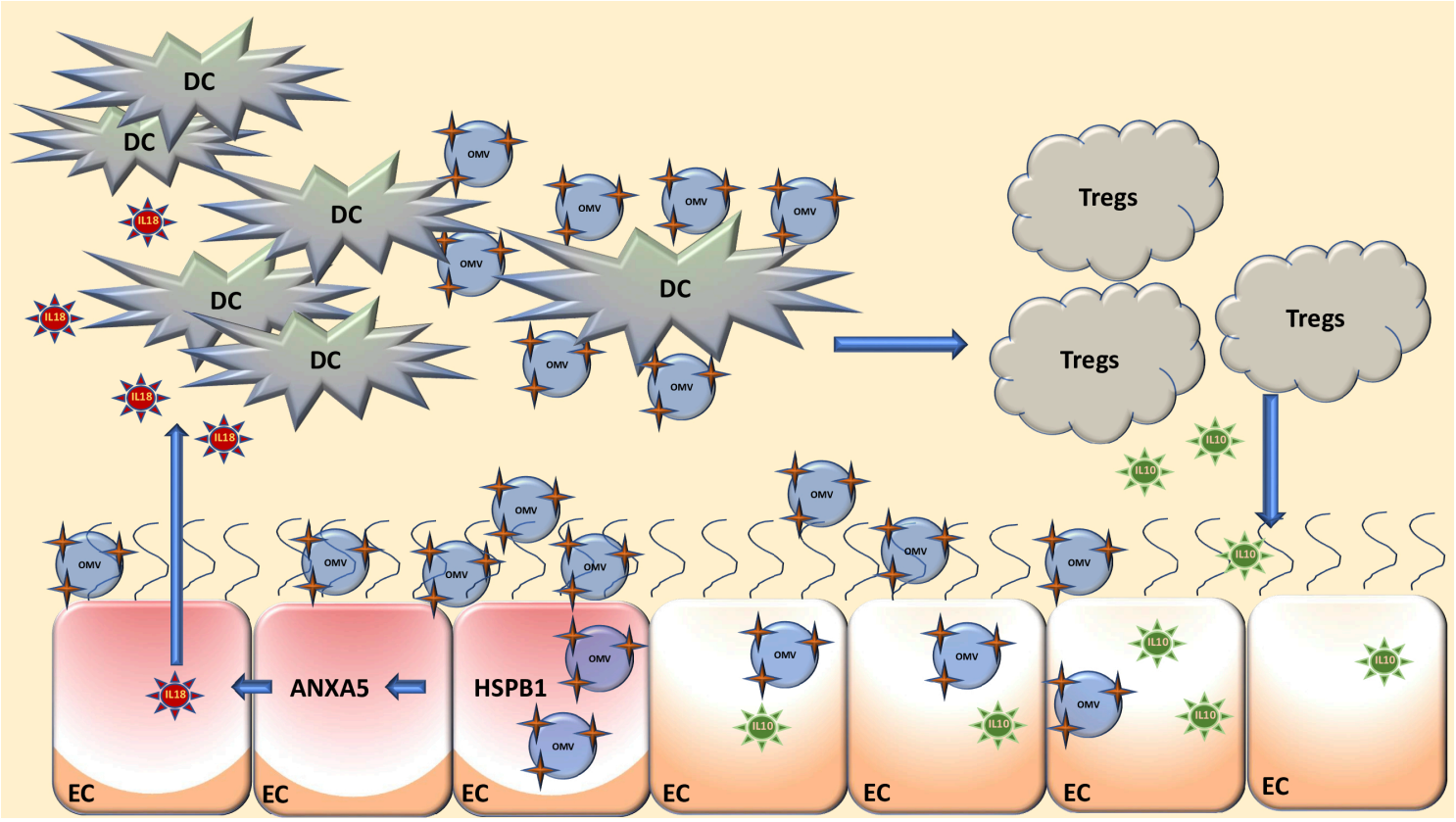


Figure 7

A possible mechanism of inflammatory response suppression in epithelial cells treated with OMVs. NTBF OMVs interact with epithelial cells and promote the cascade activation of several proteins, including HSPB1 and ANXA5, and provoke IL-18 secretion. IL-18 can play a profound role in the initiation phase of an immune response by recruiting DCs [50]. Interleukin-18-induced DCs interact with PSA located on the surface of OMVs through Toll-like receptor 2 (TLR2). Finally, DCs modulate the activity of CD4+FOXP3+regulatory T cells (Tregs), which secrete IL10 and suppress inflammation. EC - epithelial cells, DC - dendritic cells, Treg - T regulatory cells.

Supplementary Files

This is a list of supplementary files associated with this preprint. Click to download.

- FigS1.jpg
- SupplementarytableS1S5.xlsx
- FigureS1.jpg